ELSEVIER

Journal of Alloys and Compounds 452 (2008) 377–383

Journal of ALLOYS AND COMPOUNDS

www.elsevier.com/locate/jallcom

Structural study of metastable tetragonal YSZ powders produced via a sol–gel route

Céline Viazzi *, Jean-Pierre Bonino, Florence Ansart, Antoine Barnabé

CIRIMAT, Paul Sabatier University, 118 Rte de Narbonne, 31 062 Toulouse Cedex 09, France

Received 7 March 2006; received in revised form 9 October 2006; accepted 28 October 2006
Available online 8 December 2006

Abstract

Sol–gel yttria stabilized zirconia (YSZ) is investigated in this paper. The final aim is to process YSZ powders into stable slurries in order to prepare thick coatings for thermal barrier to be applied on hot turboengine components. In fact, this system is well-known for its excellent thermomechanical resistance at elevated temperatures but the relationship between these performances and the structural and microstructural characteristics of these materials is not fully understood. This paper reports a preliminary study concerning recent progress on the structural properties control of YSZ powders synthesized by sol–gel process and the main advantages of this process compared to conventional methods. As a first step towards this understanding, structural investigations of ZrO_2 doped with various $x$mol%$YO_{1.5}$ coatings, have been performed using X-ray diffraction, structural Rietveld refinement, Raman spectra analysis and transmission electron microscopy. The evolution of the crystallographic structure of YSZ powders after air annealing at various temperatures 1100 °C, 1200 °C and 1400 °C was studied to well understand the conditions of the formation of desired metastable tetragonal phase (t′). Then, this work should allow to correlate chemical and thermomechanical parameters as YSZ formulation and sol–gel elaboration conditions, temperature and t′ phase performances.

Keywords: YSZ; Crystal structure and symmetry; X-ray diffraction; Sol–gel; Metastable phase

1. Introduction

Zirconia is a widely used material thanks to its unique features. Indeed, its mechanical properties, in particular hardness and strength, combined with good optical, ionic and electrical characteristics make this material suitable for many applications such as coatings, interferometric filters [1] or solid electrolytes [2]. Such excellent properties of zirconia strongly depend on both crystal structure and phase transformations. At atmospheric pressure, pure zirconia has three solid polymorphs which exhibit monoclinic [space group $P2_1/c$], tetragonal [space group $P4_2/nmc$] and cubic [space group $Fm3m$] symmetries. The use of pure zirconia ceramics as advanced structural materials is limited due to the spontaneous tetragonal to monoclinic (t → m) phase transformation upon cooling from elaboration temperature to room temperature. This martensitic transition results in irreversible damages caused by about 4.5% volume expansion. The desire to stabilize the high temperature (tetragonal and cubic) phases to room temperature has led to a variety of oxide addition designed to lower even suppress altogether the high temperature transition(s). The most common system is yttria stabilized zirconia (YSZ). In particular, studies have revealed good mechanical properties for tetragonal YSZ. Two phenomena can be used to interpret those mechanical properties and the nature of the YSZ material can thus be defined as 'transformable' or 'not transformable'. The transformable tetragonal YSZ phase (called t) is of great interest when used as engineering ceramic material since it shows high values of strength and hardness. This hardening mechanism is due to the transformation of the tetragonal phase into the monoclinic phase which implies a volume change associated with pseudoplasticity [3,4]. The amount of yttrium is an important parameter since it has an influence on the grain size, the temperature of the martensitic transformation, strength and degradation behavior, especially in humid environment [5–7]. The 'non-transformable' metastable tetragonal YSZ phase (called t′) [8] is remarkably resistant and does not undergo the transformation to the monoclinic phase under stresses, for example. With high rate deposition techniques (EBPVD, plasma

* Corresponding author. Tel.: +33 5 61 55 02 64; fax: +33 5 61 55 61 63.
E-mail address: viazzi@chimie.ups-tlse.fr (C. Viazzi).

0925-8388/$ – see front matter © 2006 Elsevier B.V. All rights reserved.
doi:10.1016/j.jallcom.2006.10.155

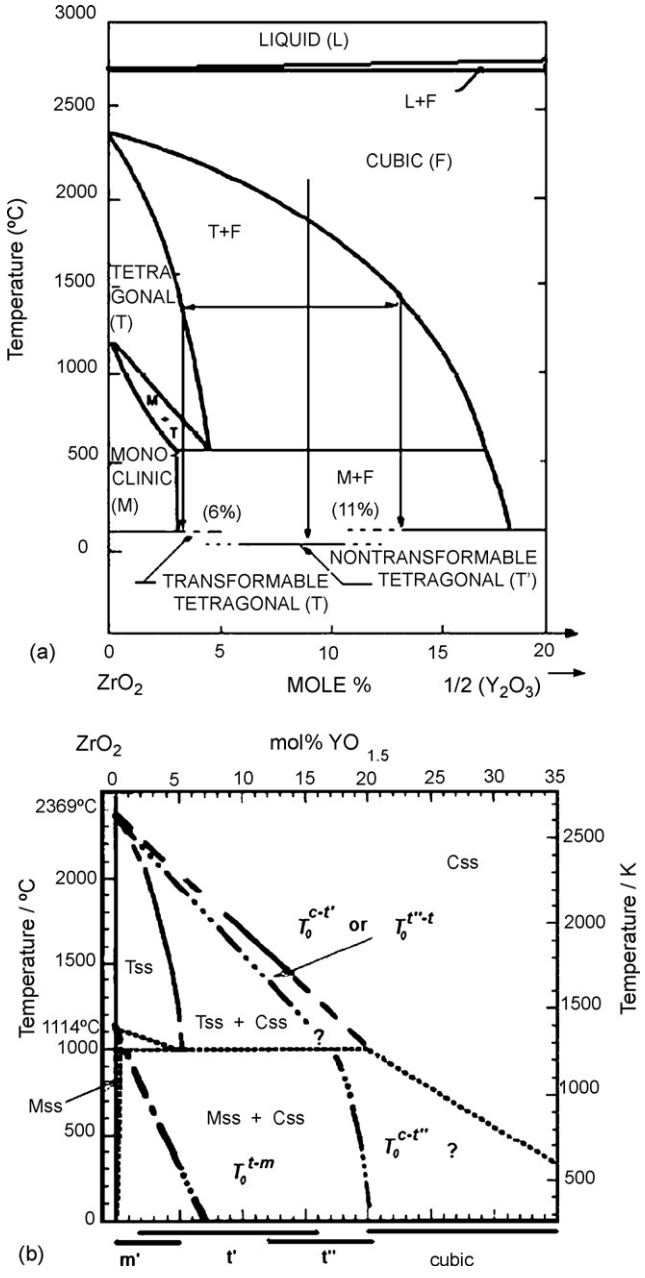

Fig. 1. (a) ZrO_2–Y_2O_3 phase diagram, after Miller et al. [11], (b) diagram including stable–metastable boundary lines after Yashima et al. [12].

spray) the t′ phase is obtained via a displacive transformation by quenching liquid or cubic phase from high temperature. The t′ phase is widely used for thermal barrier applications due to the formation of a tweed microstructure which tends to increase the thermomechanical performances [9]. This microstructure corresponds to a three-dimensional pseudo-periodic lattice of high Y_2O_3 cubic particles within all of the t′ grains [10]. However, as Miller et al. first demonstrated [11], t′ phase undergoes a phase separation by diffusion when aged at temperatures greater than 1200 °C which can allow the t → m transformation upon cooling.

According to the phase diagram proposed by the latter named authors (Fig. 1a), the domain of existence of the t phase, t, is

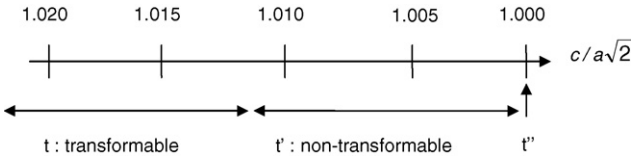

Fig. 2. The tetragonal forms of yttria stabilized zirconia.

in the range 0–6 mol%$YO_{1.5}$. The addition of yttrium to zirconia allows to obtain the 'non-transformable' phase up to about 13 mol%$YO_{1.5}$. In a more recent study, Yashima et al. [12] proposed a diagram including stable–metastable boundary lines T_0 (Fig. 1b). From a crystallographic point of view, the ratio of the cell parameters can be used to distinguish between the two tetragonal phases (t and t′). The ratio $c/a\sqrt{2}$ tends to 1.010 for the t′ cell parameters while it is superior to 1.010 for the t phase. Scott [8] has widely studied these different tetragonal phases. In the 4–13 mol%$YO_{1.5}$ range, Scott has determined the cell parameter variations as a function of the amount of $YO_{1.5}$ in mol% (x):

$$a\sqrt{2} = 0.50801 + 0.03582x, \qquad c = 0.51944 + 0.03045x$$

The existence of a third particular metastable tetragonal phase, called t″, has been pointed out by Raman spectroscopy and neutronic scattering [12]. Usual X-ray diffraction analysis does not allow to distinguish this t″ phase from a cubic phase since the cell parameters ratio of this tetragonal phase is equal to the unity. However, this crystal structure is considered as a tetragonal phase because of a slight distortion of the anionic network. The stability domains of the different tetragonal forms of YSZ versus the ratio of their cell parameters are represented in Fig. 2.

This paper presents a study based on a chemical route known as sol–gel method to obtain without quenching the YSZ metastable t′ phase. For the first time, a soft chemical process was investigated to replace physical processes such EBPVD or plasma spray. The sol–gel route is based on hydrolysis and inorganic polymerization of metal precursor. By definition, the main advantage is that this soft chemical process does not require high temperature treatments. The objective was to determine if the sol–gel route was able to synthesize YSZ powders with the same metastable tetragonal crystal structure (t′) like conventional physical processes would be able to do so [13]. Clarifying the synthesis route before the development of the sol–gel route as a processing technique is crucial in order to elaborate high temperature protective coatings supplied with good thermomechanical performances.

2. Experimental

Sols were synthesized using an alkoxide route. The precursor used was the zirconium (IV) propoxide ($Zr(OPr)_4$, 70 wt% solution in 1-propanol) and the solvent was the 1-propanol (99 + wt%). The yttrium precursor was obtained by solubilization of yttrium (III) nitrates hexahydrate (99 + wt%) in 1-propanol (99 + wt%) at a concentration of 0.5 mol L^{-1}. YSZ sols are obtained by both hydrolysis and complexation reactions. So the addition of a slight quantity of water changes the gelation kinetics. We have to notice that the reactivity of $Zr(OPr)_4$ is very fast towards water. Consequently, the complexing agent,

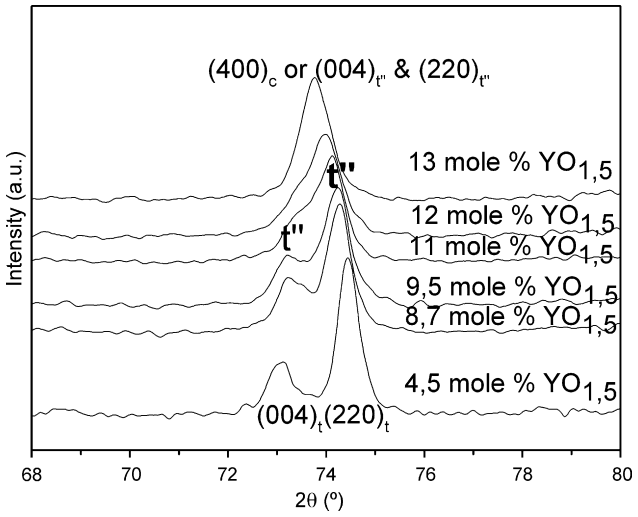

Fig. 3. Part of diffractograms of powders synthesized with varying the amount of yttrium x (mol%$YO_{1.5}$).

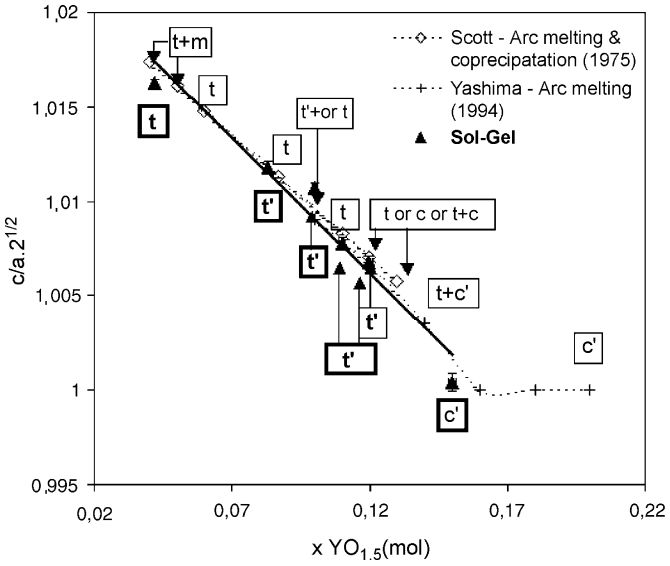

Fig. 4. Comparison of the tetragonal character of powders obtained by the sol–gel route and the results exposed in the literature. c′ indicates the presence of cubic or tetragonal metastable t″ phase, m, t and t′, respectively, indicate the presence of monoclinic, tetragonal and tetragonal metastable t′ phase. The amount x of $YO_{1.5}$ is based on the chemical analysis.

acetylacetone (AcAc), was used to decrease this reactivity. The molar ratios $AcAc/Zr(OPr)_4$ and $H_2O/Zr(OPr)_4$ were kept constant to 0.8 and 9.5, respectively.

After the gelation step at 50 °C in a dry oven, powders were heat treated 2 h at 950 °C (heating rate: 100 °C/h, cooling rate: 10 °C min^{-1} or lower). Finally, a chemical analysis by inductively coupled plasma (ICP) was carried out in order to verify the yttrium amount in the samples.

Powders were characterized by X-ray diffraction measurements and analyzed using the Rietveld method. X-ray diffraction patterns were collected at room temperature by scanning steps of 0.02° (2θ) over a $20° < 2\theta < 100°$ angular range with a θ–θ Seifert XRD 3003 TT equipped with a graphite secondary monochromator and working with a Cu Kα radiation (0.15418 nm). For the tetragonal, cubic and monoclinic phases the space groups used for Rietveld refinement were *$P4_2/nmc$* (137), *F3-3m* (225) and *$P2_1/C$* (14), respectively.

Raman spectra were obtained by using a *Labram Laser HB* spectrophotometer. A He/Ne laser was used of 632.8 nm wavelength and a power equal to 17 mW/cm^2. No luminescence problem was observed during the measurements.

Finally, observations using transmission electron microscopy (TEM) were performed with a JEOL 2010 JEM device.

3. Results and discussion

3.1. Powders characterization by XRD

Several powders were synthesized using the protocol described above and the amount of yttrium, defined as x mol%$YO_{1.5}$, was the only variable parameter. Each sample was then characterized by XRD and Fig. 3 shows a close up of the obtained diffraction patterns. No splitting is observed around the 75° (2θ) area (Fig. 3) in the case of the alloy containing 13 mol%$YO_{1.5}$ what it is expected to be the more relevant. Moreover, the ratio of its cell parameters ($c/a\sqrt{2}$) is equal to unity (Table 1). These results mean that the symmetry of the 13 mol%$YO_{1.5}$ powder is either cubic or tetragonal metastable t″.

For x in the compositional range 4.5–12 mol%$YO_{1.5}$, the XRD patterns (Fig. 3) correspond to a tetragonal crystallographic system and no mixture is observed under the detection level. The lattice cell parameters and the tetragonality ($c/a\sqrt{2}$) of the samples are presented in Table 1.

The evolution of the tetragonality ($c/a\sqrt{2}$) of the sol–gel powders versus the amount of yttria is in good agreement with previous results obtained by Scott [8] and Yashima et al. [12] as shown in Fig. 4. Their crystallographic analyses have been performed on powders obtained by arc melting or co-precipitation techniques. In both cases, high temperature preparations have been carried out: up to 1700 °C for arc melting and 24 h at 1200 °C for the co-precipitation synthesis [8]. Whatever the method of synthesis, the tetragonal character ($c/a\sqrt{2}$) decreases when the amount of yttrium increases (see Fig. 4). However, an

Table 1
Crystallographic characterization of the powders according the amount of yttrium x (mol%$YO_{1.5}$)

x (mol%$YO_{1.5}$)	Phase	Chemical analysis (mol%$YO_{1.5}$)	$\frac{[(\text{mol\%YO}_{1.5})_{\text{analysis}} - \text{mol\%YO}_{1.5}]}{(\text{mol\%YO}_{1.5})_{\text{analysis}}}$ (%)	Cell parameters (nm)	$c/a\sqrt{2}$
4.5	t	4.2 ± 0.4	7	$a = 0.3605(3)$; $c = 0.5181(2)$	1.016
8.7	t′	8.3 ± 0.8	5	$a = 0.3609(4)$; $c = 0.5164(3)$	1.012
9.7	t′	10 ± 1	3	$a = 0.3615(4)$; $c = 0.5163(3)$	1.010
11.0	t′	11 ± 2	<1	$a = 0.3617(5)$; $c = 0.5155(4)$	1.008
12.0	t′	12 ± 2	<1	$a = 0.3621(5)$; $c = 0.5155(4)$	1.007
13.0	c or t″	15 ± 2	13	$a = 0.3631(1)$; $c = 0.5137(5)$	1.000

Fig. 5. TEM observation of powder (9.7 mol%$YO_{1.5}$) obtained by sol–gel route.

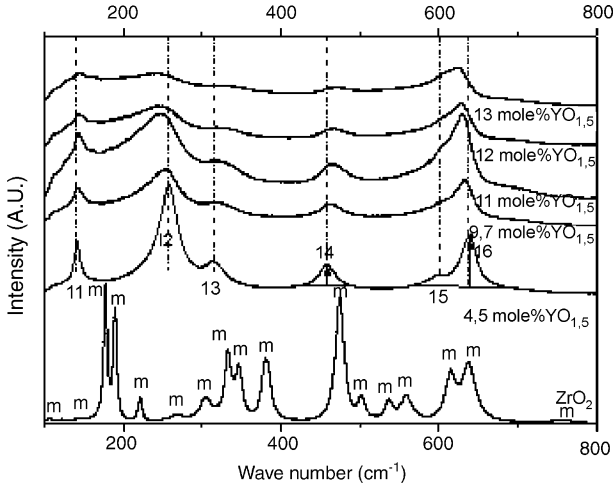

Fig. 6. Raman spectra of powders obtained by sol–gel route.

important point is that no t + m and t + t′ mixtures are observed using the sol–gel route. Moreover, it is important to emphasize that no mixture of the monoclinic and cubic phases is observed while it is predicted from the stable phase diagram (Fig. 1) at the considered temperature and for the considered range of yttria. Hence, the sol–gel route makes possible to synthesize metastable tetragonal powders as the high deposition rate techniques are able to do so. However, the phenomena involved cannot be the same since sol–gel is a soft chemistry process and it does not require high temperature set up.

Scott [8] has noticed, in the range 4–5 mol%$YO_{1.5}$, that the mixture t + m is always obtained with a variable ratio. According to this author, the grain size may have an influence on this transition. Later, other authors [14,15] have explained that under a critical grain size diameter tetragonal precipitates are stable in this structure because of the large amount of energy required to create new surface area when undergoing the t → m transformation. The sol–gel grain size certainly plays an important role in the preparation of pure tetragonal phase using this soft chemical route. An observation by TEM of powder containing 9.7 mol%$YO_{1.5}$ is shown in Fig. 5. We notice that the grain size does not exceed 40 nm when synthesized via the sol–gel route.

3.2. Raman spectroscopy

Contrary to X-ray diffraction, Raman spectroscopy is especially sensitive to the local symmetry. Indeed, this vibrational spectroscopy is sensitive both to oxygen displacements due to large polarizability [16] and to the intermediate order without the long range periodicity [17]. Fig. 6 shows the Raman spectra of the as synthesized powders.

Monoclinic zirconia has been synthesized for a reference. This monoclinic symmetry is distinguishable by 18 Raman peaks corresponding to 18 active modes. Spectra are very different in the case of yttrium substitution since the tetragonal symmetry only has six active modes. The associated peaks reported in Fig. 6 have been labeled I_1 to I_6.

For each powder, no mixture with a monoclinic phase is observed. This is in perfect agreement with the XRD analysis. However, we can notice that the intensity ratio I_4/I_6 (Fig. 7) decreases when the amount of yttrium increases. This phenomenon highlights the oxygen displacement decrease when the amount of yttrium increases. This result is in agreement with the Yashima's conclusions [12]. For 13 mol%$YO_{1.5}$, the peaks are very low. But the fact that those peaks are present indicates this is still a case of a tetragonal symmetry. In conclusion, for the sample containing 13 mol%$YO_{1.5}$ the tetragonal metastable t″ phase is present since the ratio of its cell parameters is equal to the unity, according to XRD analyses. However, we cannot conclude on the presence of a c + t″ mixture because the characteristic spectrum of the cubic symmetry in Raman spectroscopy is a large broad band.

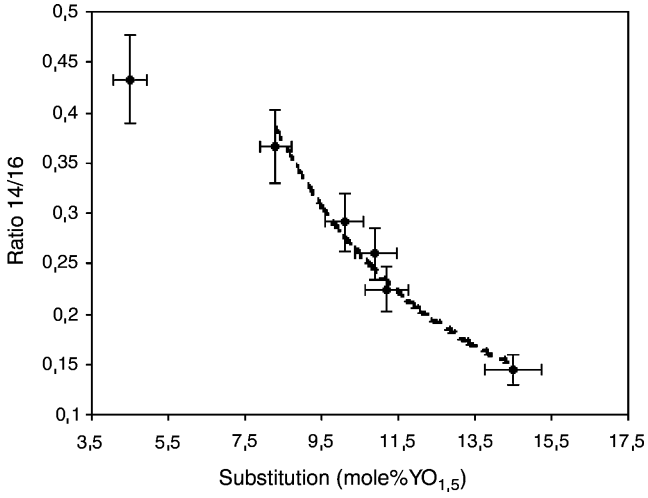

Fig. 7. Ratio I_4/I_6 for the Raman spectroscopy bands.

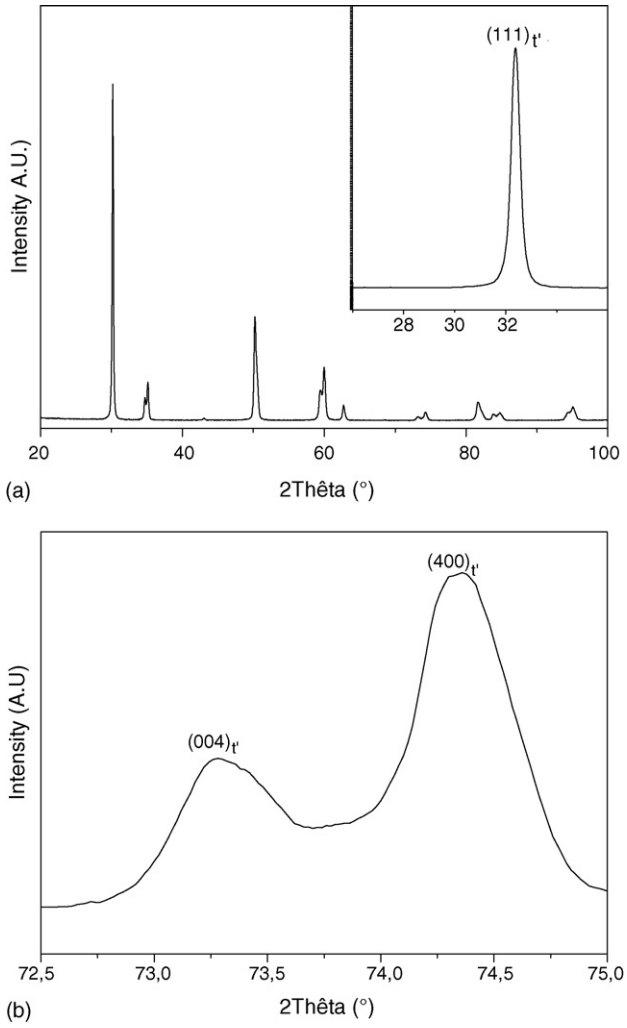

Fig. 8. (a) For 9.7 mol%$YO_{1.5}$, diffractogram obtained after a 100 h heat treatment at 1100 °C, (b) zoom on the 75° (2θ) area.

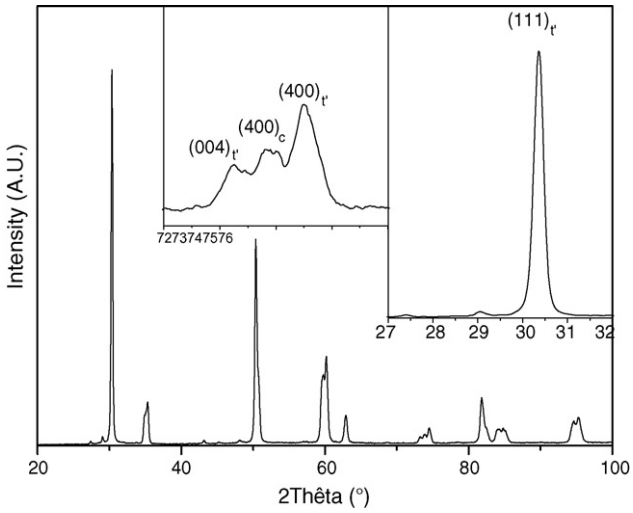

Fig. 9. For 9.7 mol%$YO_{1.5}$, diffractogram obtained after a 100 h heat treatment at 1200 °C.

3.3. Effect of heat treatments

3.3.1. Characterization of sol–gel powders by XRD analyses

Samples containing 9.7 mol%$YO_{1.5}$ were annealed at temperatures of 1100 °C, 1200 °C and 1400 °C for periods of 100 h. Sample annealing was carried out in air using an alumina crucible. Powders were then cooled overnight at 10 °C min^{-1} cooling rates (or lower) and each sample was characterized by XRD. The obtained patterns are reported in Figs. 8–10.

Even after a 100 h annealing time at 1100 °C, the tetragonal phase was still pure (Fig. 8) and no monoclinic phase was observed under the detection level. While the temperature is maintained at 1200 °C, the cubic phase was formed as demonstrated by the characteristic $(400)_c$ Bragg peak (Fig. 9). However, no monoclinic phase was observed. Finally, at 1400 °C, the system was completely destabilized and the tetragonal phase was no more observed. And only the cubic and monoclinic phases were then detected (Fig. 10). The point corresponding to 9.7 mol%$YO_{1.5}$ at 1400 °C is located near the center of the mixed tetragonal–cubic phase (see Fig. 1). So, at the equilibrium, the composition would be about 50 vol.% of cubic and tetragonal phase. An XRD quantitative analysis using Rietveld refinement was performed to determine the concentration of both monoclinic and cubic phases in the sol–gel prepared powder after firing at 1400 °C for 100 h. The results and the standard agreement factors are given in Table 2. Note that volumes are around 50% of cubic and monoclinic phases. This coincides with the expected behavior of the diffusion-controlled t′ phase separation into tetragonal (t) and cubic phase. As shown on the stable phase diagram (Fig. 1), on slow cooling, such as that we performed (10 °C min^{-1} or lower), the t′ phase evolves in a mixture of cubic phase and a lower yttria tetragonal phase (t) which is then transformed into the monoclinic phase following the general schematic expressed by: t′ → c + t → c + m. As a result, the non-transformable label may not be applicable to the formed low yttria phase t any more since it undergoes the t → m transformation. In the high yttria content region, the cubic phase is stable in temperature and remains cubic upon cooling.

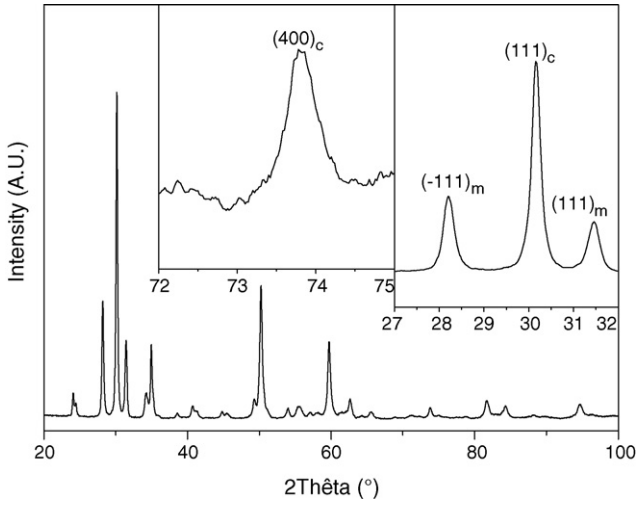

Fig. 10. For 9.7 mol%$YO_{1.5}$, diffractogram obtained after a 100 h heat treatment at 1400 °C.

Table 2
Results of Rietveld refinement of the powder obtained after a heat treatment of 100 h at 1400 °C

Crystallographic phases	Cell volume (Å^3)	Z	Scale factor	wt%	vol.%
Cubic: $a = 5.138(1)$	135.6	2	3.8459×10^{-5}	52.95	51.9
Monoclinic: $a = 5.167(2)$; $b = 5.212(2)$; $c = 5.317(2)$; $\gamma = 99.09(2)$	141.4	2	3.2785×10^{-5}	47.05	48.1

3.3.2. Comparison with previous studies and discussion

The results obtained after a 100 h thermal treatment at 1100 °C, are in perfect agreement with those obtained by physical processes (EBPVD or plasma spray) [10]. The presence of the cubic phase has been also detected by previous studies [10] after annealing at 1200 °C. However, this observation was made for longer treatments (250 h against 100 h in our case). For this duration, the cubic phase has not been identified. The grain size may have an influence and may explain this difference. However, the use of different cooling rates is another important parameter and this topic is being discussed below.

The evolution of the t′ phase in a mixture of cubic and monoclinic phases has already been observed by previous studies [18–20] after annealing at 1400 °C or higher. However, note that the experimental conditions of these studies have not been exactly the same ones. In the work of Van Valzah and Eaton [18], a sample (t′ phase) containing 7.5 wt%Y_2O_3 (8.2 mol%$YO_{1.5}$) has been aged at 1482 °C for 100 h. The ageing time carried out by Jones and Mess [19] has been 40% longer (140 h) at only 1400 °C. This heat treatment has been carried out on a sample containing 7.8 mol%$YO_{1.5}$ (t′ phase). Despite the experimental differences described above by Van Valzah and Eaton [18] and Jones and Mess [19] have found about 50 vol.% of cubic and monoclinic phases and no other phase has been identified after ageing. Finally, Brandon and Taylor [20] have characterized a sample containing 8.6 mol%$YO_{1.5}$ (t′) after ageing at 1400 °C for 100 h. The latte named authors have not precise the proportion of the monoclinic and cubic phases in the aged sample but no other phase has been detected. Two parameters are similar in the latter mentioned studies [18–20]. First, the amount of yttria is located near the center of the mixed cubic–tetragonal phase. Moreover the samples were characterized after slow cooling rates (furnace cooling). For comparison, in many studies [18,20], annealing treatments followed by rapid quenching (∼300 °C min^{-1}) have been performed to determine the t′ phase behavior at high temperatures. It appears that the cooling rates is a very important factor for the t′ phase transformation. For instance, it has been shown for particular YSZ content that the proportion of the monoclinic phase is less important when the samples is quenched than when firing at 1400 °C for 100 h [18,20]. More precisely, for 8 wt%Y_2O_3 (8.6 mol%$YO_{1.5}$), Brandon and Taylor [20] have shown that a rapid cooling rate gives rise to a mixture of the cubic (45 vol.%) and tetragonal (55 vol.%) phases. In comparison, after furnace cooling (∼2 °C min^{-1}) the system evolves in a mixture of the monoclinic and cubic phases only.

In their study, Van Valzah and Eaton [18] have compared the effect of the cooling rate (rapid quenching or furnace cooling) on the amount of the monoclinic phase in a sample containing 7.5 wt%Y_2O_3 (8.2 mol% $YO_{1.5}$). Whatever the aging conditions (temperature/time) the amount of monoclinic phase is higher when a slow cooling rate is carried out. Moreover, an important point is that, even if the samples are rapidly quenched, the amount of the monoclinic phase increases when samples are exposed at 316 °C for 1 h. Indeed, a sample quenched after ageing at 1482 °C for 100 h showed an increase from 12.2 to 50.0 vol.% of the monoclinic phase after the low temperature heat treatment [18]. Thus, quenching followed by a low temperature treatment and a short time exposure, generate approximately the same amount of monoclinic phase as observed in the material furnace cooled from the same ageing condition (50.0 and 48.4 vol.%, respectively). Lughi and Clarke have also observed the same phenomenon the t′ phase transformation in monoclinic phase at low temperatures [21,22]. Samples (8.6 mol%$YO_{1.5}$) annealed for 195 h, 125 h and 75 h at 1425 °C and rapidly quenched (∼300 °C min^{-1}) evolved over time at low temperatures (including room temperature). These authors have shown that the monoclinic phase develops under such conditions and the transformation is faster for coatings annealed for 195 h at 1425 °C and proceeds slower in coatings annealed for shorter times (125 h and 75 h). This further emphasizes the instability of the quenched-in tetragonal phase.

4. Conclusions

Metastable tetragonal YSZ powders were prepared by sol–gel route and the evolution of their tetragonal symmetry, $c/a\sqrt{2}$, versus the amount of yttria is similar to the ratio corresponding to materials obtained by arc melting and co-precipitation at higher temperatures. Indeed, the addition of yttrium allows a better control of the amount of the stable tetragonal t phase, then tetragonal metastable t′ and, finally, tetragonal metastable t″ YSZ phase. Moreover, by this synthesis method, no m + t and t + t′ mixtures were observed contrary to the other processes.

Heat treatments during 100 h at 1100 °C, 1200 °C and 1400 °C, followed by furnace cooling, showed that the crystallographic evolutions for the sol–gel powder containing 9.7 mol%$YO_{1.5}$ and of materials obtained by physical processes with high rate of deposition (EBPVD/plasma spray) are the same. However, the phenomena are different. Indeed, t′ phase can be obtained by rapid quenching from the cubic phase. In the case of a sol–gel process, no high temperature is required. Nevertheless, the formation of the t′ phase can be explained by the small grain size due to the excellent homogeneity of precursors in the sol. For comparison, Garvie et al. [23] have shown that it is possible to synthesize tetragonal zirconia if the grain size does not exceed 5 nm. This phenomenon can be explained

by the main effect of the surface energy compared to the bulk energy.

Thus, it is planned to determine the microstructural evolution of aged YSZ powder obtained via the sol–gel route. The aim would be to compare the mechanisms involved into the t′ phase transformation using such technique with those undergone by the t′ phase obtained by rapid quenching from the cubic or liquid phase.

This sol–gel process, original for such TBC applications seems to be very attractive because it is a low cost technology and because of its easiness to be integrated into an industrial process.

Acknowledgements

This work results from a grant given by the French DGA (Delegation Generale de l'Armement) and the CNRS. The authors would like to thank these organisms for their support.

References

[1] H.A. Mcleod, Thin Film Optical Filter, 2nd ed., Adam Hilger, Bristol, 1986, p. 519.
[2] P. Lenormand, D. Caravaca, Ch. Laberty-Robert, F. Ansart, J. Eur. Ceram. Soc. 25 (2005) 2643.
[3] I. Nettleship, R. Stevens, Int. J. High Tech. Ceram. 3 (1987) 1.
[4] E.C. Subbarao, Adv. Ceram. 3 (1981) 1.
[5] F.F. Lange, J. Mater. Sci. 17 (1982) 240.
[6] T. Masaki, J. Am. Ceram. Soc. 69 (1986) 638.
[7] T. Masaki, Ceram. Int. 13 (1993) 109.
[8] H.G. Scott, J. Mater. Sci. 10 (1975) 1527.
[9] R. Mevrel, C. Rio, M. Poulain, C. Diot, F. Nardou, Technical Report No. 28/2019M, ONERA, 1987.
[10] L. Lelait, Thesis, University of Orsay, France, 1991.
[11] R.A. Miller, J.L. Smialek, R.G. Garlic, J. Am. Ceram. Soc. 3 (1981) 241.
[12] M. Yashima, M. Kakihana, M. Yoshimura, Solid States Ionics 86 (1996) 1131.
[13] C. Viazzi, F. Ansart, J.P. Bonino, Proceeding of the Poudres et Matériaux Frittés 2005, Cherbourg, France, 2005.
[14] D.L. Porter, A.H. Heuer, J. Am. Ceram. Soc. 60 (1977) 183.
[15] T.K. Gupta, F.F. Lange, J.H. Betchtold, J. Mater. Sci. 13 (1978) 1464.
[16] C. Kittel, Introduction to Solid State Physics, 2nd ed., Dunod, Paris, 1970.
[17] K. Matsui, H. Susuki, M. Oghai, H. Arashi, J. Ceram. Soc. Jpn. 98 (1990) 1302.
[18] J.R. Van Valzah, H.E. Eaton, Surf. Coat. Technol. 46 (1991) 289.
[19] R.L. Jones, D. Mess, Surf. Coat. Technol. 86 (1996) 94.
[20] J.R. Brandon, R. Taylor, Surf. Coat. Technol. 46 (1991) 75.
[21] V. Lughi, D.R. Clarke, Surf. Coat. Technol. 200 (2005) 1287.
[22] V. Lughi, D. Clarke, J. Am. Ceram. Soc. 88 (2005) 2552.
[23] R.C. Garvie, R.H. Hannink, R.T. Pascoe, Nature 258 (1975) 703.